Heliyon 10 (2024) e35800

Contents lists available at ScienceDirect

Heliyon

journal homepage: www.cell.com/heliyon

Research article

Yishen Huazhuo decoction regulates microglial polarization to reduce Alzheimer's disease-related neuroinflammation through TREM2

Kai Wang [a,1], Shujie Zan [b,1], Jiachun Xu [a,1], Weiming Sun [a], Caixia Li [c], Wei Zhang [b], Daoyan Ni [a], Ruzhen Cheng [b], Lin Li [b], Zhen Yu [d], Linlin Zhang [a], Shuang Liu [a], Yuanwu Cui [e], Yulian Zhang [a,*]

[a] *The Second Affiliated Hospital of Tianjin University of Traditional Chinese Medicine, Tianjin, 300250, China*
[b] *Tianjin University of Traditional Chinese Medicine, Tianjin, 301617, China*
[c] *Tianjin Key Laboratory of Acute Abdomen Disease Associated Organ Injury and ITCWM Repair, Institute of Acute Abdominal Diseases of Integrated Traditional Chinese and Western Medicine, Tianjin Nankai Hospital, Nankai Clinical College, Tianjin Medical University, Tianjin, 300100 China*
[d] *Department of Encephalopathy, Tianjin Academy of Traditional Chinese Medicine Affiliated Hospital, Tianjin 300120, China*
[e] *Shenzhen Traditional Chinese Medicine Treatment Hospital, Shenzhen, 518100, China*

ARTICLE INFO

Keywords:
Alzheimer's disease
Yishen Huazhuo decoction (YHD)
Neuroinflammation
Microglial polarization
TREM2

ABSTRACT

Background: Aging is the primary risk factor for the onset of Alzheimer's disease (AD). Inflamma-aging is a major feature in the process of aging, and the chronic neuroinflammation caused by inflamma-aging is closely related to AD. As the main participant of neuroinflammation, the polarization of microglia (MG) could influence the development of neuroinflammation.
Objective: This study aims to observe the impact of YHD on microglia (MG) polarization and neuroinflammation to delay the onset and progression of AD.
Methods: In vivo experiment, four-month senescence accelerated mouse prone 8 (SAMP8) were used as the model group, the SAMR1 mice of the same age were used as the control group. In YHD group, 6.24 g/kg YHD was intragastrically administrated continuously for 12 weeks, and Ibuprofen 0.026 g/kg in positive control group. Morris Water Maze test was used to evaluate the learning and memory ability, Nissl's staining and immunofluorescence double staining for neuron damage and MG M1/M2 polarization, Enzyme-Linked Immunosorbent Assay (ELISA) for neuroinflammation biomarkers in hippocampus, Western blot for key protein expression of TREM2/NF-κB signaling pathway. In vitro experiments, 10 μM/l $A\beta_{1\text{-}42}$ induced BV-2 cell model was used to re-verify the effect of YHD regulating MG polarization to reduce neuroinflammation. Also, TREM2 small interfering RNA (siRNA) was used to clarify the key target of YHD.
Results: YHD could improve the learning and memory ability of SAMP8 mice evaluated by the Morris Water Maze test. Like Ibuprofen, YHD could regulate the M1/M2 polarization of MG and

Abbreviations: AD, Alzheimer's disease; Arg-1, arginase 1; Aβ, β-amyloid peptides; CNS, central nervous system; HPLC, high-performance liquid chromatography; IL-1β, interleukin-1β; IL-10, interleukin-10; IL-6, interleukin-6; iNOS, inducible nitric oxide synthase; IKKβ, inhibitor of kappa B kinase β; MG, microglia; NF-κB, nuclear factor-κB; NFTs, Neurofibrillary tangles; PU.1, Purine-rich box1; SAMP8, senescence accelerated mouse prone 8; SAMR1, senescence accelerated mouse resistant 1; siRNA, small interfering RNA; TNF-α, tumour necrosis factor-α; TREM2, triggering receptor expressed on myeloid cells 2; YHD, Yishen Huazhuo Decoction.

* Corresponding author.
E-mail address: zhyl220@126.com (Y. Zhang).
[1] Equal contribution to this paper.

https://doi.org/10.1016/j.heliyon.2024.e35800
Received 21 February 2024; Received in revised form 29 July 2024; Accepted 5 August 2024
Available online 6 August 2024

the levels of neuroinflammatory markers TNF-α and IL-10 in hippocampus, and relieve neuroinflammation and neuron loss. In addition, YHD could also regulate the expression of PU.1, TREM2, p–NF–κB P65 in the TREM2/NF-κB signaling pathway. Further in vitro experiments, we found that YHD had a significant regulatory effect on $A\beta_{1\text{-}42}$-induced BV-2 cell polarization, and it could significantly increase PU.1, TREM2, decrease p–NF–κB P65, *p*-IKKβ, TNF-α, IL-6, IL-1β. At the same time, using siRNA to inhibit TREM2, it proved that TREM2 was a key target for YHD to promote $A\beta_{1\text{-}42}$-induced BV-2 cell M2 polarization to reduce neuroinflammation.
Conclusions: YHD could regulate the TREM2/NF-κB signaling pathway through TREM2, thereby to adjust MG polarization and reduce AD-related neuroinflammation.

1. Introduction

Alzheimer's disease (AD), a degenerative disorder in central nervous system (CNS) occurred in the senescence phase and old period, mainly manifests as progressive cognitive and memory dysfunction. The two typical pathological features of AD are senile plaque formed by local β-amyloid peptides (Aβ) deployment and Neurofibrillary tangles (NFTs) formed by abnormal phosphorylation of Tau protein [1]. In addition, neuroinflammation is also one of the important pathological characteristics of AD, and it is considered an important cause of cognitive loss and neural degeneration related to age [2]. Highly insoluble Aβ and NFTs and damaged neurons can act as obvious inflammatory stimuli to induce neuroinflammation, making it run through the entire pathological process of AD [3,4]. Excessive neuroinflammation can aggravate the excessive production and aggregation of Aβ and abnormal phosphorylation of Tau protein [5,6], to further damage the neurons and form a vicious cycle. It suggests that neuroinflammation is a key upstream mechanism for the development of AD [7], and it might delay the development of AD to reduce neuroinflammation as soon as possible.

Neuroinflammation in CNS is mainly driven by microglia (MG) activation disorders [8], which is the abnormal proportion between M1 type MG with inflammatory effects and M2 type MG with anti-inflammatory effects. The M1 type MG is related to the expression of iNOS, which can promote the inflammatory response and increase the damage of the neuron; while the M2 type MG is related to the expression of Arg-1, which can antagonize the inflammatory response to prevent the death of neurons [9]. Studies have shown that the intervention of MG activation and its related inflammatory signals at the early stages can prevent the development of neurodegenerative diseases [10]. Triggering receptor expressed on myeloid cells 2 (TREM2), an important gene factor of AD [11,12], mainly expressed in MG in CNS, could regulate the MG from M1 to M2 polarization, alleviate neuroinflammation induced by Aβ [13] and enhance the ability of MG to remove Aβ [14]. Therefore, it could promote MG M2 polarization by regulating the TREM2 signaling pathway to reduce the early excessive neuroinflammation of AD.

Yishen Huazhuo Decoction (YHD) is a traditional Chinese medical compound, consisting of Yinyanghuo (*Epimedium*), Nvzhenzi (*Fructus Ligustri Lucidi*), Heshouwu (*Radix Polygoni Multiflori*), Roucongrong (*Cistanche*), Chuanxiong (*Ligusticum wallichi Franchat*), and Shichangpu (*Acorus gramineus*). Our previous study has proved that it could improve the learning and memory ability of the senescence accelerated mouse prone 8 (SAMP8), and the medium dose (6.24 g/kg) showed the most obvious effects [15]. YHD could promote the clear of $A\beta_{1\text{-}42}$ by regulate autophagy to improve the memory loss of the 7-month-old SAMP8 mouse [16]. However, it is not clear whether YHD could regulate MG polarization to reduce AD-related neuroinflammation. Therefore, in this study, the four-month-old SAMP8 mouse and immortalized mouse microglia (BV-2) were selected to explore the potential mechanism of YHD by reducing neuroinflammation and delaying the memory loss of AD with in vivo and in vitro experiments.

2. Material and methods

2.1. Medicine preparations

YHD comprised the following Chinese herbs: Yinyanghuo (*Epimedium*) 10 g, Nvzhenzi (*Fructus Ligustri Lucidi*) 10 g, Heshouwu (*Radix Polygoni Multiflori*) 6 g, Roucongrong (*Cistanche*) 10 g, Chuanxiong (*Ligusticum wallichi Franchat*) 6 g, and Shichangpu (*Acorus gramineus*) 6 g. All the single herbs in the formula were provided and standardized for active main compounds by the Second Hospital Affiliated to Tianjin University of Traditional Chinese Medicine. The traditional Chinese medicine decoction was refluxed and filtered, extracted and concentrated, frozen and dried, and crushed into the YHD lyophilized powder, sealed and stored in a cool and dry place for reserve. This process means that 48 g medicinal materials can be prepared into 14.4 g freeze-dried powder, with a concentration ratio of 3.3. Ibuprofen, a clinical common nonsteroidal anti-inflammatory drug, was purchased from Harbin Pharmaceutical Group Shiyitang CO., Ltd.

2.2. HPLC for the active components of YHD

According to the *Chinese Pharmacopoeia*, one or more standard ingredients were selected for each Chinese herb. The control products were precisely referred and 50 % methanol configured controlling solution were added. The quality concentration of each component was 56 μg/ml of Epimella, 6 μg/ml of Ferulic acid, 9.6 μg/mL of nuezhenoside, 30.4 μg/ml of 2,3,5,4′-tetraxyl hydroxylene-2-O-β-D-glucoside, 37.2 μg/mL of Echinacoside, 8.4 μg/ml of Verbascoside. The Acorus gramineus was extracted and determined by water. Take 0.1g YHD lyophilized powder, add 50 % ethanol ultrasound to extract 40 min, absorb the supernate, filter with 0.45 μm

microporous filter membrane, and prepare the test solution for the filter liquid. High-Performance Liquid Chromatography (HPLC) (Agilent 1260 Infinity, USA) was used to determine the components.

2.3. Animals and treatments

45 four-month-old male SAMP8 mice of SPF grade and 15 SAMR1 mice, weighing 25–30 g, all provided by the First Affiliated Hospital of Tianjin University of Traditional Chinese Medicine (SCXK(Jin) 2015–0003) were used in this study. They were raised in a single cage for each mouse in the Animal Center of Tianjin Nankai Hospital, with 12 h light-dark alternating, room temperature 23–25 °C, relative humidity (50–60) %. During the experiment, all animal procedures were approved by the local ethical committee in the Tianjin University of Traditional Chinese Medicine (TCM-LAEC2020105) and met the guidelines of the Guide for the Care and Use of Laboratory Animals published by the National Institutes of Health. 45 SAMP8 mice were randomly divided into model (P8) group, YHD group and Ibuprofen group, 15 in each group, with 15 SAMR1 mice as control (R1) group. The dosage of YHD for mice was 6.24 g/kg per day,calculated by raw material of herbs 48 g/70 kg (human body weight) × 0.0026/20 g (conversion coefficient for humans and mice). The corresponding YHD lyophilized powder was weighed at a concentration ratio of 3.3 and mixed with distilled water to make the corresponding concentration of the drug solution, which was given to the YHD group mice by gavage once a day for 12 weeks. The dosage of Ibuprofen for mice was 0.026 g/kg per day, calculated by 0.2 g/70 kg (human body weight) × 0.0026/20 g (conversion coefficient for humans and mice). The corresponding dosage of Ibuprofen granules was prepared with distilled water to make the corresponding concentration of the drug solution for Ibuprofen group by gavage once daily for 12 weeks. The mice in P8 and R1 group were given the same volume of distilled water by gavage.

2.4. Morris Water Maze (MWM) test

After the end of the last intragastric administration, the learning and memory ability was tested using MWM, as described previously [16]. In the MWM test, each mouse in all groups started with the place navigation trial for 5 consecutive days, at entry points according to a semirandom protocol. The mouse was allowed to swim for 65 s until it found the submerged platform and stayed on the platform for a maximum of 10 s. If the mouse failed to find the hidden platform within 65 s, it would be guided to the platform and remained on the platform for a maximum of 10 s. The escape latency (the time taken to search for the platform within 65 s), swimming speed, and swimming path were recorded by the tracking system. The spatial probe test was conducted 24 h after the place navigation trial. The platform was removed and the mice were placed in water according to the water entry point in the established plan. The number of times the mouse crossing the original platform area and the entire movement track was recorded within 65 s. After 65 s, the software automatically stopped recording, and the mice were taken out and dried.

2.5. Nissl's staining

The hippocampal tissue sections were cultured with Nissl's staining solution (Beyotime, Shanghai, China) for 5 min, washed with distilled water and dehydrated with 95 % ethanol. The morphology and arrangement of hippocampal CA1 cells were observed under a 400 × light microscope (Nikon, Japan). Neurons were counted with Image-Pro Plus 6.0.

2.6. $A\beta_{1\text{-}42}$ oligomer preparation

$A\beta_{1\text{-}42}$ (Aladdin, Shanghai, China) was fully dissolved in HFIP for 1 mM/l, and then transferred to a polyethylene centrifugation tube after spinning to incubate 2 h to gather $A\beta_{1\text{-}42}$. It was then centrifugated 800 *g* in room temperature in vacuum conditions until the peptide membrane appearing at bottom. The dried $A\beta_{1\text{-}42}$ peptide membrane can be stored at −80 °C, and it can be completely dissolved to 5 mM/l by DMSO when in use. Finally, the solution was diluted to 500 μM/l with sterile PBS, whirled for 30 s, and the $A\beta_{1\text{-}42}$ Oligomer could be obtained after incubation for 24 h.

2.7. Cell culture and transfection

The BV-2 cells (CL-0493) were kindly provided by Wuhan Pricella Biotechnology Co.,Ltd, which had been tested for the absence of mycoplasma and authenticated by short tandem repeats (STR) profiling method (Supplementary 1). They were cultured in high sugar DMEM medium (Cytiva, Utah USA) with 10 % fetal bovine serum (VivaCell, Shanghai, China) and 1 % penicillin/streptomycin (Solarbio, Beijing, China), in 5 % CO_2, 37 °C. The siRNA transfection was conducted under the guidance of reagent manufacturers. Control siRNA or TREM2 siRNA (SYNBIO, Suzhou, China) was incubated for 20 min in room temperature in a serum medium with MegaTran 2.0 Transition Reagent (Origene, Rockville, MD, USA). The transfection mixture was cultured for 24 h. TREM2 siRNA transfection sequences were as follows.

hs-TREM2-si-1: sense 5′-AGAACACCUGACAACUUCUdTdT-3′, antisense 5′-AGAAGUUGUCAGGUGUUCUdTdT-3';
hs-TREM2-si-2: sense 5′-GGUAAGAACACCUGACAACUUdTdT-3′, antisense 5′-AAGUUGUCAGGUGUUCUUACCdTdT-3';
hs-TREM2-si-3: sense 5′-GAGCCUCUUGGAAGGAGAAAUdTdT-3′, antisense 5′-AUUUCUCCUUCCAAGAGGCUCdTdT-3'.

Table 1
Primers used for qRT-PCR analysis.

Gene	Forward sequence 5′-3′	Reverse sequence 5′-3′
PU.1	5′CGACACCTTTCTCTCTCGGC3′	5′GGCACCATGGGAGTATCGAG3′
TREM2	5′TGGGTCACCTCTAGCCTACC3′	5′AACTTGCTCAGGAGAACGCA3′
GAPDH	5′TGGCCTTCCGTGTTCCTAC3′	5′GAGTTGCTGTTGAAGTCGCA3′

2.8. Cell counting Kit-8 (CCK-8) assay

The BV-2 cells were seeded on the 96-well plate, and the number of cells was 5×10^3/holes. Different concentrations of YHD (0, 1, 2.5, 5, 10, 25, 50, 100 μg/ml) or $A\beta_{1\text{-}42}$ (0, 0.625, 1.25, 2.5, 5, 10, 20, 40 μM/l) were used to separately treat BV-2 cells for 24 h. Also, different concentrations of YHD (0, 1.25, 5, 10, 25, 50, 100, 200 μg/ml) were added in $A\beta_{1\text{-}42}$ induced BV-2 cell model for 24 h. After 10 μl cell counting Kit-8 solution (Beyotime, Shanghai, China) was added for 4 h of incubation, the microplate reader was used to determine the absorbance at 450 nm. Live cell percentage calculation formula was: cell vitality (%) = [(A450 treatment-A450 blank)/(A450 control-A450 blank)] × 100.

2.9. Determination of lactate dehydrogenase (LDH) release

The BV-2 cells were seeded on the 96-well plate, and the number of cells was 5×10^3/holes. The release of LDH into the culture medium was measured by cytotoxicity LDH Assay Kit-WST (Dojindo Molecular Technologies, Japan) according to the manufacture's protocol. Absorbance at 490 nm was recorded and used to index LDH activity. The ratio of LDH activity in the supernatant to total LDH activity was calculated and presented as the percentage of cell death.

2.10. Immunofluorescence double staining

The sliced hippocampus tissue or fixed BV-2 cells were sealed with 5 % normal sheep serum at room temperature for 1 h, and then incubated overnight at 4 °C with primary antibodies iNOS (ab210823, abcam, 1:200), Arg-1 (#2435, CST, 1:200). They were rinsed with PBS 3 times at room temperature on the next day, and then fluorescent second antibody (A11035/A11029, Invitrogen, 1:1000) were added to incubate for 2 h with avoiding light. They were then rinsed with PBS 3 times and the excess water was absorbed with filter paper. After adding the buffer glycerin, they were covered with block sealing. Fluorescent microscope (Leica, German) was used to observe the specific fluorescent strength and take pictures. The nucleus was blue, and iNOS and Arg-1 were marked as green and red, respectively. Image-J software was used for analysis.

2.11. Western blot

Total protein was collected from mouse hippocampus or BV-2 cells to detect protein concentrations. The protein sample was separated by SDS-PAGE, and then transferred to the PVDF membrane (Millipore, USA). After closing with 5 % skimmed milk, primary antibodies were added to detect PU.1 (#2258, CST, 1:1000), TREM2 (#76765, CST, 1: 1000), p–NF–κB P65 (#3033S, CST, 1:1000), *p*-IKKβ (#2694, CST, 1:1000), GAPDH (#5174, CST, 1:1000), β-actin (#3700, CST, 1:1000), incubated overnight at 4 °C, and then incubated for 2 h at room temperature with second antibody (BS13278/BS12478, Bioworld, 1:50000). The chemical luminous substrate kit (Affinity Biosciences, Jiangsu, China) was used for color rendering, and Chemidoc XRS system (BIO-RAD, USA) for imaging, Quantity One for assessing band and semi-quantitative analysis.

2.12. Enzyme-Linked Immunosorbent Assay (ELISA)

After obtaining mouse hippocampus tissue or BV-2 cells culture supernatants, the content of inflammation-related cytokines IL-6, TNF-α, IL-1β, and IL-10 was detected according to the instructions of the kit (abs520004, abs 520010, abs 520001, abs 520005, Absin).

2.13. Quantitative real-time PCR (qRT-PCR) analysis

BV-2 cells total RNA was extracted using the Trizol reagent (Beyotime, Shanghai, China) according to the manual, and then the total RNA was reversed to cDNA using PrimeScript RT reagent Kit (Takara, Japan). Finally, the target gene expression was detected by Go Taq® qPCR Master Mix kit (Promega, Wisconsin, USA), and the primer sequence was listed in Table 1. The mRNA value of the targeted gene is described by the relative intensity of GAPDH with endogenous genes. The nucleotide sequences of the primers used in this study were showed in Table 1.

2.14. Statistical analysis

The results were expressed as Mean ± SD or Median (IQR) and SPSS 19.0 software was used for statistical analysis. For repeated measures data (escape latency), repeated measure analysis of variance was used. For data meeting normal distribution, one-way

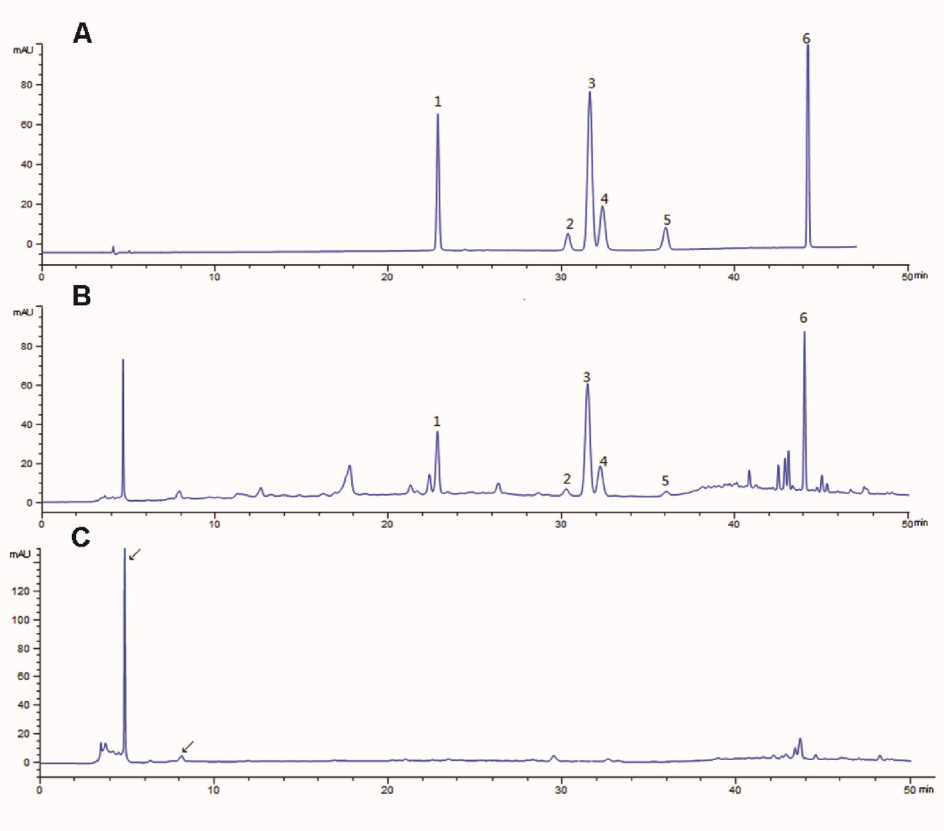

Fig. 1. Typical chromatograms of mixed standard compound (A), YHD lyophilized powder (B) and Shichangpu (*Acorus gramineus*) water solution (C). 1.Echinacoside, 2.Verbascoside, 3.2,3,5,4-Tetrahydroxystilbene-2-O-β-D-glucoside, 4.Ferulicacid. Ligustroflavone, 6.Icariin.

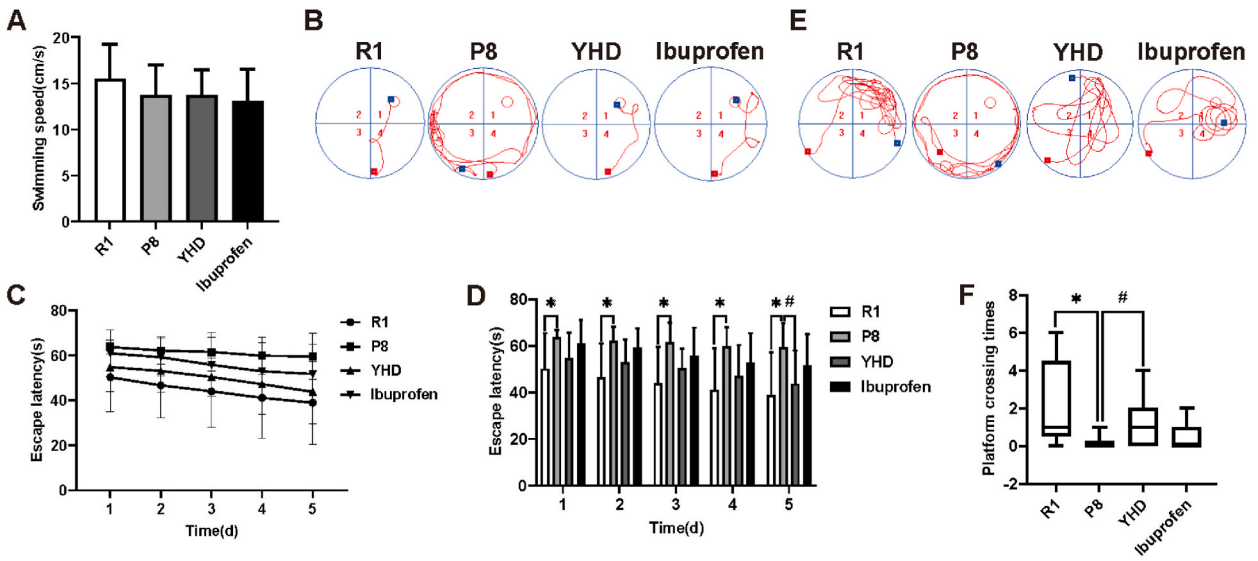

Fig. 2. YHD improves the learning and memory ability of SAMP8 mice in MWM. (A) Swimming speed on the first day. (B) Swimming path in the navigation experiment on the fifth day. (C, D) Escape latency changes of each group. (E) Swimming path in the spatial probe test. (F) The numbers of platform crossing. The number of crossing platforms are expressed as Median (IQR), swimming speed and escape latency are expressed as Mean ± SD (n = 15), $^{*}P < 0.05$ vs R1 group; $\#P < 0.05$ vs P8 group.

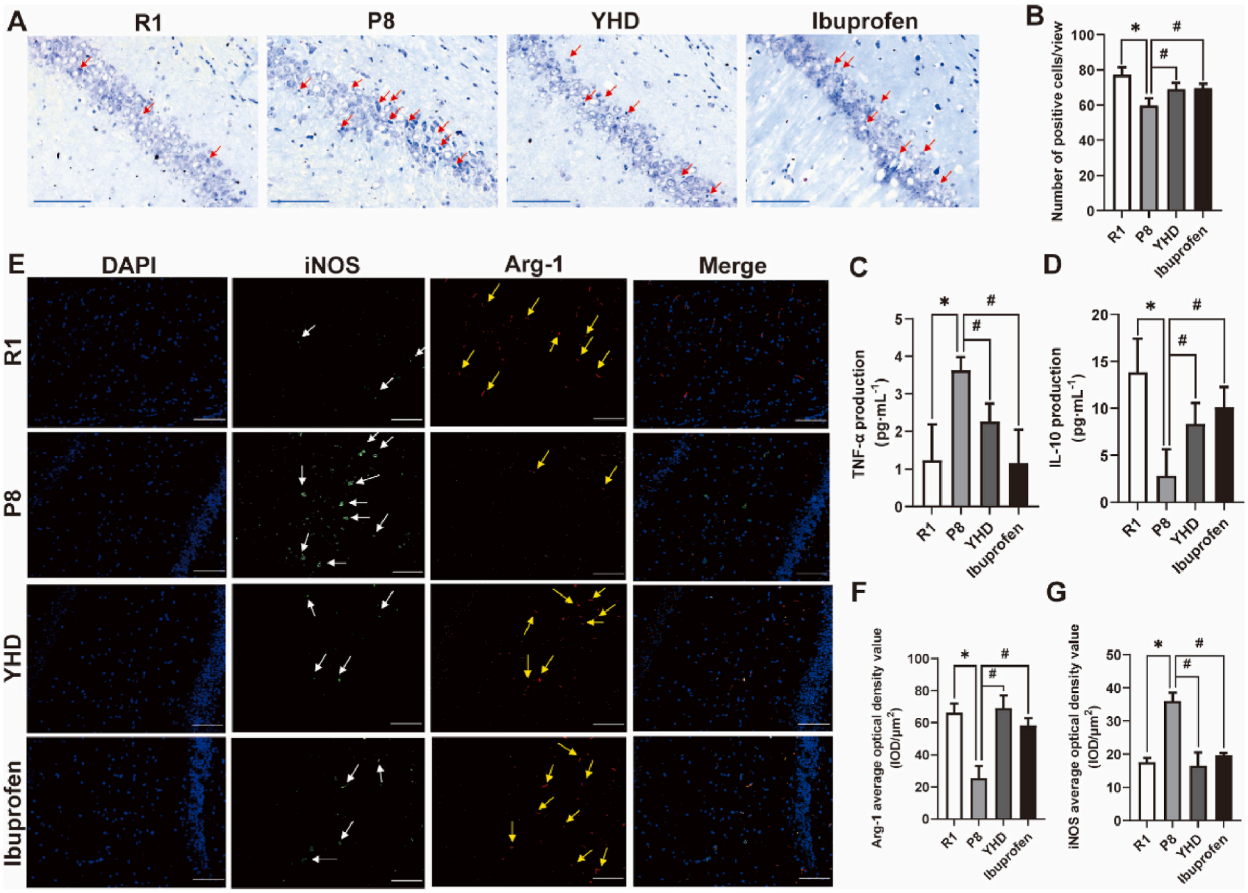

Fig. 3. Influence of YHD on M1/M2 polarization, neuroinflammation and neuron loss in hippocampus of SAMP8 mice. (A) The Nissl's staining results of the neurons in hippocampal CA1 area (scale bar = 50 μm), the red arrow indicating the lack of neurons. (B) Quantifications of neuron count in hippocampal CA1 area. (C, D) The ELISA test results of TNF-α and IL-10. (E) The immunofluorescence double staining results of MG in hippocampal CA1 area (scale bar = 100 μm). Blue fluorescence indicating nucleus, green fluorescence for iNOS (white arrow), and red fluorescence for Arg-1 (yellow arrow). (F, G) Quantifications of the average optical density value of iNOS and Arg-1. The data are represented by Mean ± SD (n = 3), *$P < 0.05$ vs R1 group; #$P < 0.05$ vs P8 group.

analysis of variance was used, and LSD or Dunnet T3 was used for post hoc multiple comparisons. For data not meeting normal distribution, Kruskal-Wallis was used. $P < 0.05$ indicated statistically significant.

3. Results

3.1. HPLC determination of the active components of YHD

6 corresponding components in YHD lyophilized powder were detected, as shown in Fig. 1A and B. The result showed that the contents of the investigated analytes were as follows: 2.476 mg/g of Echinacoside, 0.419 mg/g of Verbascoside, 2.550 mg/g of 2,3,5,4-Tetrahydroxystilbene-2-O-β-D-glucoside, 0.463 mg/g of Ferulicacid, 0.210 mg/g of Ligustroflavone. 4.054 mg/g of Icariin. Shichangpu (*Acorus gramineus*) was determined by water solution extraction, as shown in Fig. 1C. It was initially judged that the ingredient of Shichangpu (*Acorus gramineus*) was in 4.8 min and 8.1 min in YHD lyophilized powder.

3.2. YHD improving learning and memory ability of SAMP8 mouse

On the first day of the MWM test, there was no significant difference in the swimming speed of each group (Fig. 2A). The results of trajectories and orientation navigation experiment (Fig. 2B–D) on the fifth day showed that the escape latency gradually shortened, and the decline trend was roughly the same among the whole groups. Compared with the R1 group, the escape latency for P8 group increased significantly. However, on the fifth day, the escape latency in YHD group shortened significantly compared with that in the P8 group. Space navigation test and the 6th day's motion trajectory indicated that the number of crossing platform of P8 group was significantly less than the R1 group (Fig. 2E and F). But after YHD treatment, the number of SAMP8 mice across the platform could

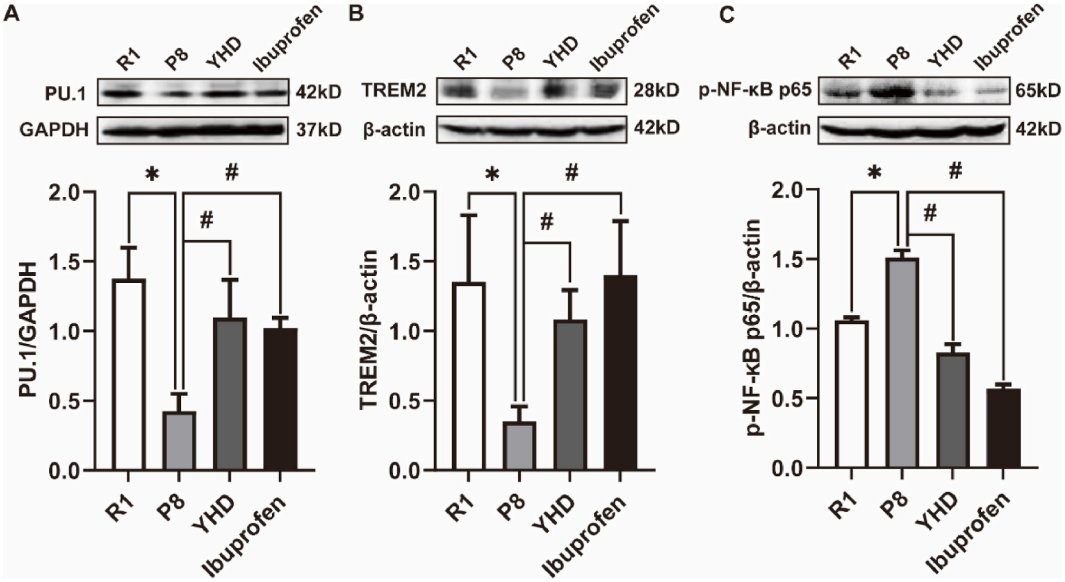

Fig. 4. Influence of YHD on PU.1, TREM2, and p–NF–κB p65 proteins in hippocampus of SAMP8 mice. The data are represented by Mean ± SD (n = 3), *$P < 0.05$ vs R1 group; #$P < 0.05$ vs P8 group.

significantly increase. while in the Ibuprofen group, the result was not significantly difference from that in P8 group in the navigation experiment and probe trials. Therefore, the above results confirmed that YHD treatment could effectively improve the learning and memory ability of SAMP8 mice.

3.3. Influence of YHD on M1/M2 polarization of microglia, reducing neuroinflammation, improving neuron loss in SAMP8 mice hippocampus

Hippocampus is a key area responsible for memory and cognition, and the loss of neurons in the CA1 area of the hippocampus is an important pathological basis that causes learning and memory decline of AD model mouse. We observed the influence of YHD on the morphology of neurons in CA1 area of SAMP8 mice (Fig. 3A and B). The results showed that compared with R1 group, the neurons in the P8 group were more disordered, with much more irregular or ruptured dead cells, and the number of neurons decreased significantly. After the treatment of YHD and Ibuprofen, the loss of neurons in the SAMP8 mice had been improved to a certain extent.

The hippocampus neuron injury of SAMP8 mice is closely related to neuroinflammation, so we tested TNF-α and IL-10 expression in hippocampus by ELISA (Fig. 3C and D). The results showed that compared with R1 group, the TNF-α content in P8 group increased significantly, and IL-10 decreased significantly. After the treatment of YHD or Ibuprofen, the release of TNF-α significantly reduced, while IL-10 increased significantly in SAMP8 mice, indicating a comprehensive function in reducing neuroinflammation.

MG is an important cell participating in neuroinflammation and neuronal damage, and the type of MG polarization determines the direction of neuroinflammation. In order to observe the influence of YHD on MG polarization, we used immunofluorescence double staining to detect the expression of MG M1 polarization marker (iNOS) and MG M2 polarization marker (Arg-1) of the hippocampus (Fig. 3E–G). The results showed that compared with R1 group, the iNOS expression in P8 group increased significantly, and the Arg-1 expression decreased significantly. While both YHD and Ibuprofen could significantly decrease the expression of iNOS, increase Arg-1 expression in SAMP8 mice, to promote MG M2 polarization.

3.4. YHD regulating proteins of TREM2/NF-κB signaling pathway of SAMP8 mouse

TREM2 is an important regulatory factor for MG function. PU.1 plays a direct control of TREM2 gene transcription in the upstream. In order to explore the mechanism of MG activation by YHD, we first detected the two key regulatory factors of MG functions, PU.1 and TREM2 (Fig. 4A and B). The Western blot results showed that compared with R1 group, the expression of PU.1 and TREM2 in P8 group significantly reduced, and after the treatment of YHD and Ibuprofen, the expression of PU.1 and TREM2 significantly increased in SAMP8 mice.

We have proved that YHD could improve neuroinflammation by regulating the release of TNF-α and IL-10. p–NF–κB P65, a key protein for regulating the inflammatory response, could induce the expression of multiple inflammatory cytokines and inflammatory mediators. Several studies have confirmed that TREM2 could inhibit inflammatory cytokines release by regulating NF-κB signaling pathway [17]. Therefore, we measured the expression of p–NF–κB P65 protein (Fig. 4C). The Western blot results showed that compared with R1 group, the expression of p–NF–κB P65 protein in P8 group significantly increased, and after the treatment of YHD and Ibuprofen, the expression of p–NF–κB P65 protein significantly reduced in SAMP8 mice. Therefore, the above results indicated that

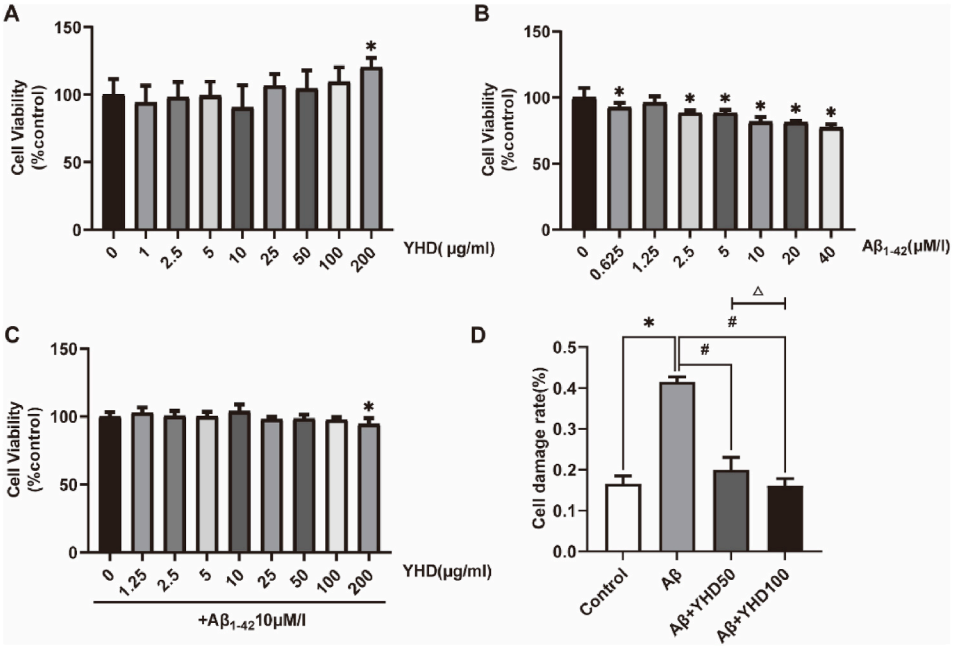

Fig. 5. YHD reducing the toxic effect of $A\beta_{1\text{-}42}$ on BV-2 cells. (A) CCK-8 method to detect the vitality of BV-2 cells after YHD treatment. (B) CCK-8 detection of the vitality of BV-2 cells after treated by $A\beta_{1\text{-}42}$. (C) Using 10 μM/l $A\beta_{1\text{-}42}$ to induce BV-2 cells to establish cell models, and CCK-8 method to detect the effects of YHD on the vitality of cell models. (D) The effects of 50 μg/ml and 100 μg/ml YHD on the LDH release of BV-2 cells after treated by10 μM/l $A\beta_{1\text{-}42}$. The data are represented by Mean ± SD (n = 3), $^*P < 0.05$ vs control group; $\#P < 0.05$ vs Aβ group; $\triangle P < 0.05$ vs Aβ+YHD50 group.

YHD might regulate the TREM2/NF-κB signaling pathway to regulate MG polarization and reduce neuroinflammation, and the key molecular targets of its role were still unclear, so we continued to conduct the further in vitro experiments.

3.5. *YHD reducing the toxic effect of $A\beta_{1\text{-}42}$ on BV-2 cells*

In order to determine the compatibility of YHD and BV-2 cells, we adopted the CCK-8 method to determine the impact of YHD on the vitality of BV-2 cells at a concentration of 1–200 μg/ml (Fig. 5A). In the concentration range of 1–100 μg/ml, YHD did not significantly reduce cell vitality. We used different concentrations of $A\beta_{1\text{-}42}$ to treat BV-2 cells, and the CCK-8 results showed (Fig. 5B), as the $A\beta_{1\text{-}42}$ concentration increased, the vitality of the cells gradually decreased. After 10 μM/l treatment, the cell vitality decreased significantly by 20 %. While under other concentrations, the cell damage was lighter or severe, so the 10 μM/l $A\beta_{1\text{-}42}$ was selected as a model-making concentration. In addition, we also studied the impact of YHD on $A\beta_{1\text{-}42}$ (10 μM/l 24 h) treated BV-2 cell vitality (Fig. 5C). The results also showed that less than 100 μg/ml YHD could not significantly impact on BV-2 cell vitality. So in subsequent experiments, we chose the YHD concentration of 50 μg/ml and 100 μg/ml. The LDH detection results found that (Fig. 5D), compared with the control group, $A\beta_{1\text{-}42}$ enhanced the release of the BV-2 cell LDH, which could be significantly reduced after YHD treatment, and the YHD high dose group was better than that in low dose group. The above results showed that YHD could reduce the toxic effect of $A\beta_{1\text{-}42}$ on BV-2 cells.

3.6. *YHD influencing the activation of BV-2 cells induced by $A\beta_{1\text{-}42}$ and reducing inflammation*

In order to explore the effects of YHD on the activation of BV-2 cells induced by $A\beta_{1\text{-}42}$, we first performed morphological observation through inverted optical microscope (Fig. 6A). The results showed that the BV-2 cells in the control group was small, mostly circular or fusiform in shape, with slender processes. After $A\beta_{1\text{-}42}$ induced, the BV-2 cells appeared significantly activated, and the cell body became larger, with thicker and short processes, in Amoeba-like shape. After treatment with different concentrations of YHD, the BV-2 cell morphological changes caused by $A\beta_{1\text{-}42}$ could be reduced to a certain extent. In addition, the ELISA results of proinflammatory cytokines (Fig. 6B–D) showed that YHD could significantly inhibit the increase levels of TNF-α, IL-6, and IL-1β of BV-2 cells induced by $A\beta_{1\text{-}42}$. The above results showed that YHD could influence the activation of BV-2 cells induced by $A\beta_{1\text{-}42}$ and alleviate inflammatory reaction.

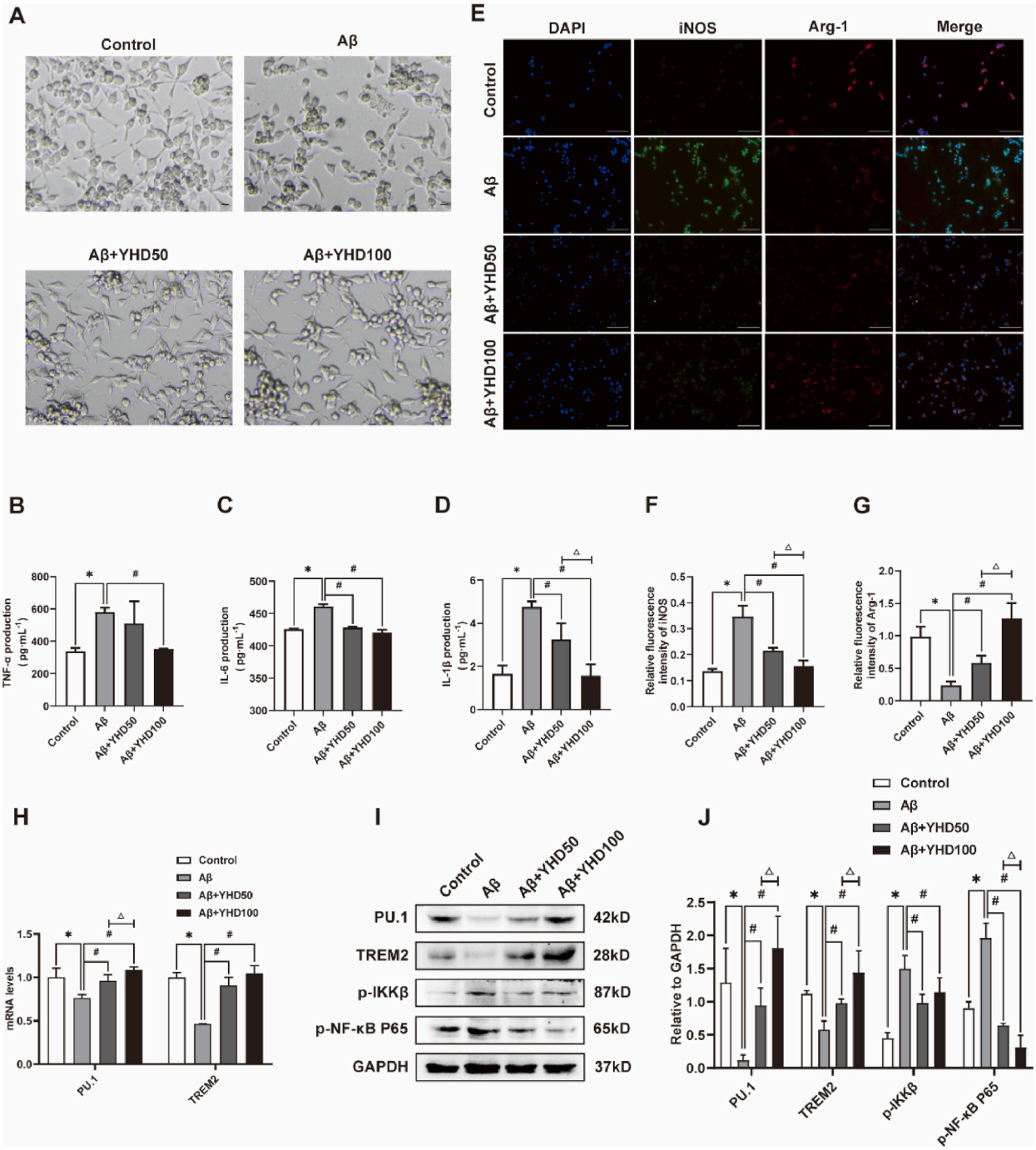

Fig. 6. YHD inhibiting the activation of BV-2 cells induced by $A\beta_{1\text{-}42}$ and promoting its polarization from M1 to M2. (A) Inverted optical microscope of BV-2 cells (scale bar = 100 μm). (B–D) The ELISA test results of TNF-α, IL-1β, and IL-6 (E) BV-2 cells immunofluorescence double-stained results (scale bar = 100 μm). Blue fluorescence indicating the nucleus, green fluorescent for iNOS, and red fluorescence for Arg-1. (F, G) Quantifications of the relative fluorescence density of iNOS and Arg-1. (H) The mRNA expression of PU.1 and TREM2 in BV-2 cells by qRT-PCR. (I, J) Quantification of protein expression levels of PU.1, TREM2, *p*-IKKβ, p–NF–κB P65 in BV-2 cells by Western blot. The data are represented by Mean ± SD (n = 3), $^*P < 0.05$ vs control group; $\#P < 0.05$ vs Aβ group; $\triangle P < 0.05$ vs Aβ+YHD50 group.

3.7. YHD regulating M1/M2 polarization and reducing inflammation by regulating TREM2/NF-κB signaling pathway in BV-2 cells induced by $A\beta_{1\text{-}42}$

we have further observed BV-2 cell polarization by immunofluorescence double staining (Fig. 6E–G). The results showed that in the

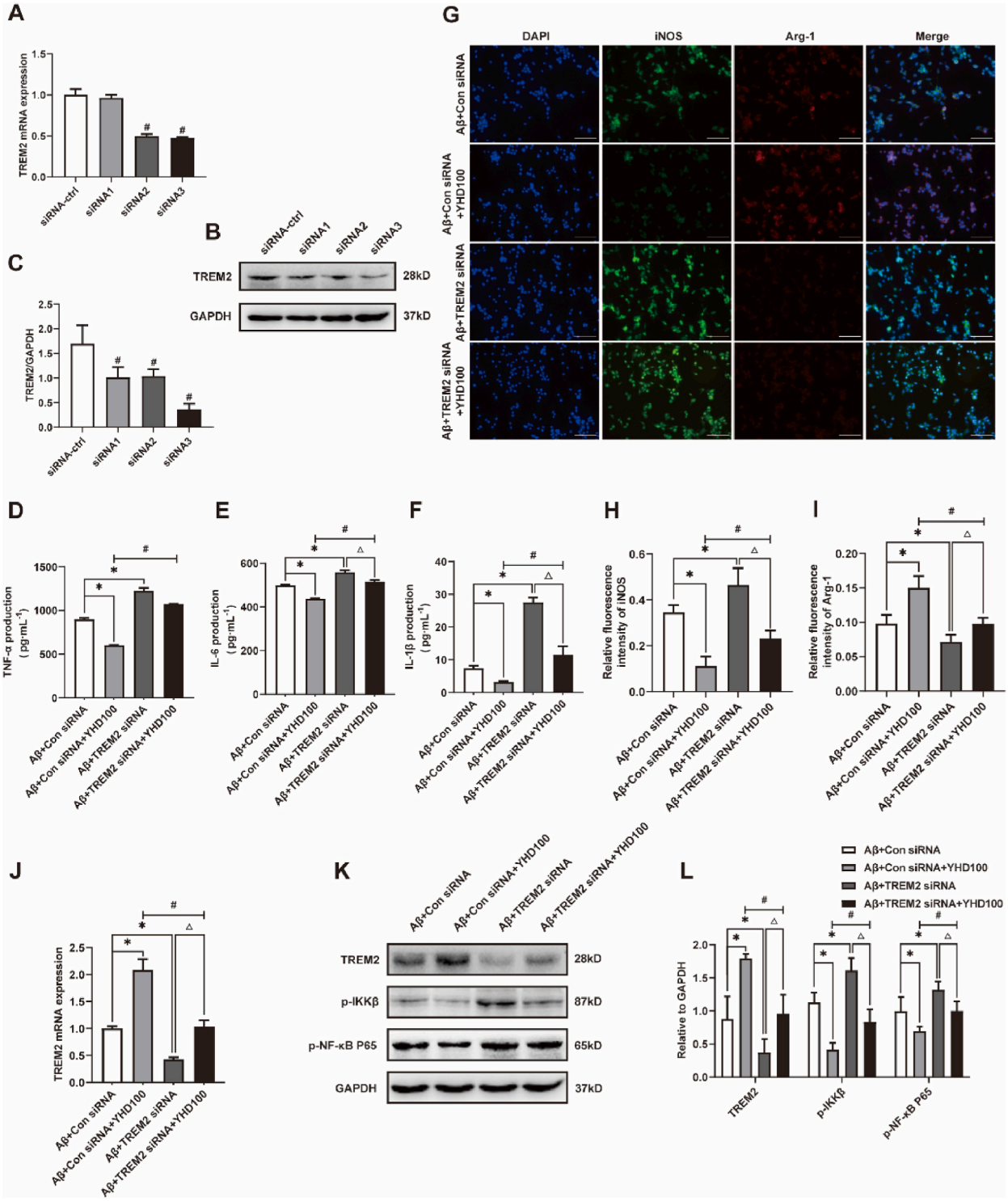

Fig. 7. TREM2 siRNA transfection partially reversed the effect of YHD improving BV-2 cells polarization and neuroinflammation. (A–C) Western blot and qRT-PCR for TREM2 by Control siRNA and different TREM2 siRNA transfection. (D–F) The ELISA test results of TNF-α, IL-1β, and IL-6. (G) The immunofluorescence double staining results of $A\beta_{1\text{-}42}$-induced BV-2 cells after jointly treated by 100 μg/ml YHD and TREM2 siRNA (scale bar = 100 μm). Blue fluorescence indicating the nucleus, green fluorescent for iNOS, and red fluorescence for Arg-1. (H, I) Quantifications of the relative fluorescence density of iNOS and Arg-1. (J) qRT-PCR for TREM2 mRNA of $A\beta_{1\text{-}42}$-induced BV-2 cells after jointly treated by 100 μg/ml YHD and TREM2 siRNA. (K, L) Quantification of protein expression levels of TREM2, *p*-IKKβ, p–NF–κB P65. The data are represented by Mean ± SD (n = 3), $^{*}P < 0.05$ vs Aβ+Con siRNA group; $\#P < 0.05$ vs Aβ+Con siRNA + YHD100 group; $\triangle P < 0.05$ vs Aβ+TREM2 siRNA group.

control group, BV-2 cells mainly manifested as M2 polarization, and $A\beta_{1\text{-}42}$ could induce BV-2 cells to M1 polarization. After treatment with different concentrations of YHD, the BV-2 cell polarization induced by $A\beta_{1\text{-}42}$ could be changed to M2 polarization. In order to further explore the mechanism of YHD regulating M1/M2 polarization of BV-2 cells induced by $A\beta_{1\text{-}42}$, we detected the expression of the TREM2/NF-κB signaling pathway (Fig. 6H–J). The qRT-PCR results showed that YHD could significantly inhibit the decrease of PU.1 and TREM2 mRNA expressions in BV-2 cells induced by $A\beta_{1\text{-}42}$. Western blot results also showed that YHD could significantly inhibit the decrease of PU.1 and TREM2 proteins in BV-2 cells induced by $A\beta_{1\text{-}42}$, and the increase the protein levels of p–NF–κB P65, *p*-IKKβ.

Based on the above results, in order to determine whether TREM2 was the main molecular target of YHD, we further verified it by using TREM2 siRNA to down-regulate TREM2. First, in order to find the appropriate cell transfection model, we used control siRNA and different TREM2 siRNA to transfect BV-2 cells. Western blot and qRT-PCR results showed that TREM2-siRNA3 was the most effective for down-regulating TREM2 protein and mRNA in BV-2 cells (Fig. 7A–C), so it was used as a subsequent cell transfection model. The results showed that (Fig. 7D–L), TREM2 siRNA significantly promoted M1 polarization of BV-2 cells induced by $A\beta_{1\text{-}42}$, significantly reduced the expression of TREM2 mRNA and protein, and significantly increased the protein levels of p–NF–κB p65 and *p*-IKKβ, thereby significantly promoted the secretion of pro-inflammatory cytokines TNF-α, IL-6 and IL-1β. However, TREM2 siRNA significantly attenuated YHD's promotion of M2 polarization and inhibition of inflammation in $A\beta_{1\text{-}42}$-induced BV-2 cells. The above results showed that YHD might promote M2 polarization of BV-2 cells induced by $A\beta_{1\text{-}42}$ and reduce inflammation by regulating the TREM2/NF-κB signaling pathway.

4. Discussion

Aging is the greatest risk factor of neurodegenerative diseases, such as AD. The aging cannot be considered a disease, but it could form a chronic low-level sterile inflammation, which is called inflamm-aging [18]. Studies have found that aging could cause important changes in brain, manifested as a significant increase in MG activation, supplemental factors and inflammatory mediators as the brain atrophy [19], to eventually induce neuroinflammation. Neuroinflammation plays a double-edged sword function during the onset of AD. It is a normal protective response to threatening stimuli, but the neuroinflammatory response should not last too long. Inflammatory and cytotoxic factors released by chronic neuroinflammation could damage the neurons [20]. Therefore, chronic neuroinflammation is considered to be a key factor that affects normal aging to mild cognitive impairment, and then the progress of AD [21]. Excessive neuroinflammation has been found to start 20 years before AD symptoms appear [5].

As a classic natural accelerated aging model mouse, SAMP8 mouse is considered to be a potential animal model for studying both aging changes and early AD changes [22]. SAMP8 mouse shows age-related learning and memory impairment, and has been proved to have pathological features similar to AD patients, such as early accumulation of Aβ, increased tau phosphorylation, abnormal glial cell response [23], and aging-related neuroinflammation [24]. Previous studies showed that SAMP8 mouse had accelerated-aging since four-mouth old, with learning and memory disorders [25,26], and MG proliferation and chronic inflammation in hippocampus occurred with the growth of the mice [23]. In this study, four-mouth old SAMP8 mice were selected to accept early intervention, and SAMR1 and other normal animals with similar physiological indicators and survival time were used as normal control. The study revealed that 4-month-old SAMP8 mice, 12 weeks after the start of the experiment, exhibited AD-related spatial learning ability and memory loss in the MWM test. The content of neuroinflammation markers of ELISA results showed aging-related neuroinflammation characteristics [27]: an increase of anti-inflammatory cytokine, IL-10, and a decrease of inflammatory cytokine, TNF-α. The YHD intervention could reduce the decline in learning memory by reducing neuroinflammation. In addition, it was also found that the perception of SAMP8 mice about changes in the breeding environment was more sensitive to easily attack each other. Also, the smoothness of hair in SAMP8 mice was not as good as that in SAMR1 mice, and with the increase of the month, the hair was rough, with different degrees of hair removal and skin ulceration in the torso and limbs. The response and sensitivity was slowed over time in SAMP8 mice. After YHD intervention, the hair removal was reduced, with smooth fur, flexible performers, and quick response, which suggested that YHD could improve the appearance and activity during the aging process of SAMP8 mice.

MG is the main factor in controlling the CNS immune response. The immune-related receptor expressed in MG participates in immune surveillance, antigen recognition and presence, phagocytic function of Aβ and other harmful substances, and the secretion of immune effect factors [28]. The immune response driven by MG participates in Aβ clearance, but with the development of the disease, the excessive neuroinflammation response of MG increased the pathological process of AD. As the main functional executor of neuroinflammation, MG can be divided into inflammatory types, M1 type that could promote inflammatory factor, accompanied by damaged phagocytic function, and anti-inflammatory types, M2 type that could secret anti-inflammatory factors and nutritional factors to improve inflammation. The M1/M2 dynamic transformation imbalance induces the occurrence of neuroinflammation. During the AD process, Aβ deposition and Tau protein abnormal phosphate can induce M1 type MG to participate in neuroinflammation by inhibiting M2 type MG [29]. Studies have confirmed that by promoting MG polarization from M1 to M2, it could reduce the adverse effects of neuroinflammation to play a neuroprotection effect on AD [30]. It is worth noting that there is evidence that at the early stage of AD, MG in the patient's brain appeared significantly activated [31,32]. While MG in the elderly brain is functional damaged, which is easier to continue to be activated [33], making the inflammatory response amplified [34]. Therefore, in the early stage of the aging process, to reduce neuroinflammation by regulating MG activation to avoid excessive inflammation caused neuron damage, it could greatly control the occurrence and development of AD. There is increasing evidence that non-steroidal anti-inflammatory drugs (NSAIDs) may be useful in reducing the risk of AD [35]. Ibuprofen is a NSAIDs, and some studies have found that Ibuprofen can effectively reduce MG activation, inflammatory response and Aβ deposition in the brain of APP transgenic mice [36]. Our study mainly aimed at neuroinflammation in the brain, so it was used as a positive control. Although NSAIDs could

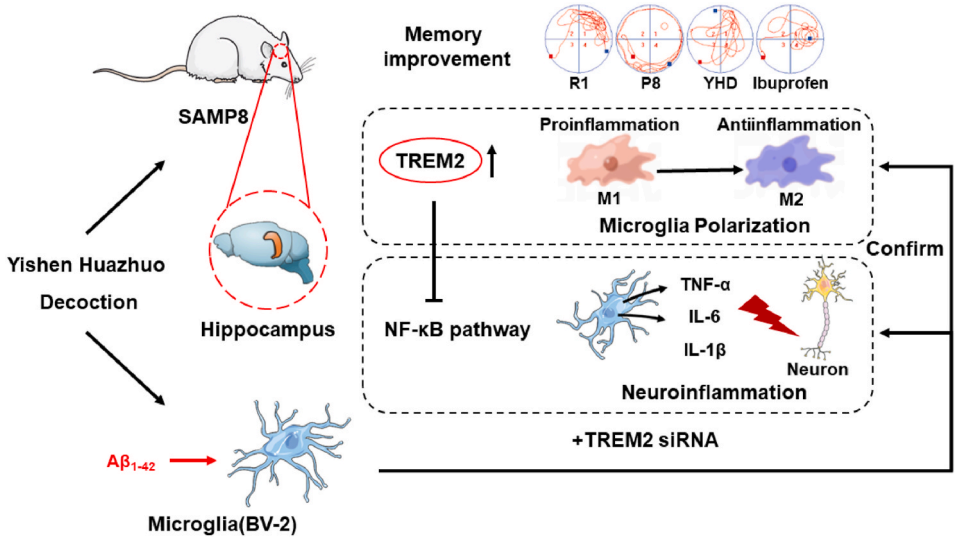

Fig. 8. Schematic diagram depicting that YHD can regulate the TREM2/NF-κB signaling pathway through TREM2, thereby to adjust MG polarization and reduce AD-related neuroinflammation, and ultimately playing a role in neuroprotection and delaying learning and memory ability decline.

reduce neuroinflammation, clinical trials have not consistently demonstrated significant improvements in cognitive function [37]. Similarly, in our study, Ibuprofen did not show better improvements in learning and memory compared to YHD. This might be due to the complex and diverse pathological mechanisms of AD, which are not solely dependent on the regulation of neuroinflammation. Our previous research also found that YHD, as a compound with comprehensive effects, could promote neuronal autophagy and reducing apoptosis in SAMP8 mice [16], which made YHD better in behavioral improvement.

In vivo experiment, by Nissl's staining and immunofluorescent double staining, we found that YHD and Ibuprofen could both promote MG polarization from M1 to M2 to reduce neuroinflammation to protect neurons in hippocampus of SAMP8 mice. The results provided a pathological basis for YHD to improve SAMP8 mice learning and memory ability. Over-expression of Aβ is often one of the important factors that promote chronic inflammation in the brain [38]. In order to further clarify the impact of YHD on MG, we chose $A\beta_{1\text{-}42}$ to induce BV-2 cells as a cell model of AD-related neuroinflammation. Similar to the previous results [39,40], through phase contrast microscopy and fluorescence microscopy, we observed that $A\beta_{1\text{-}42}$ can cause BV-2 cells to activate mainly as M1 polarization, and also increase the expression of IL-1β, IL-6, and TNF-α. YHD intervention could change the polarization of BV-2 cells under the influence of $A\beta_{1\text{-}42}$, promote it to M2 polarization, reduce the release of inflammatory cytokines, and the results once again confirm that YHD could reduce neuroinflammation by regulating MG polarization.

TREM2, the key congenital immune receptor of MG, can reduce the secretion of inflammatory cytokines and play a neuroprotective effect [41]. Moreover, TREM2 plays an important role in regulating MG polarization and alleviating neuroinflammation caused by MG [42]. In this study, we used TREM2 siRNA to inhibit the effect of TREM2 on BV-2 cells. It was found that TREM2 siRNA also blocked the function of YHD at the same time, to promote M1 polarization, and inhibit M2 polarization of BV-2 cells. The results indicated that TREM2 played an important role in regulating M1/M2 polarization of YHD. NF-κB signaling pathway is important for mediating inflammatory reactions, which is closely related to inflamma-aging [43]. TREM2 can regulate MG to release inflammatory cytokines through NF-κB signaling pathway to influence neuroinflammatory reactions [44]. The results of this study found that YHD could significantly inhibit the expression of key protein p–NF–κB P65 protein and *p*-IKKβ protein in the NF-κB signaling pathway, reduce the release of downstream inflammatory factor TNF-α, IL-6, and IL-1β. While TREM2 siRNA partially reversed the above role of YHD, suggesting that the mechanism of YHD regulating MG polarization and reducing neuroinflammation might be adjusted through the TREM2/NF-κB pathway. Traditional Chinese medicine compound has the characteristics of multi-components and multi-targets. Due to the existence of the blood-brain barrier, some of the components of traditional Chinese medicine are difficult to effectively penetrate or reach the effective concentration. However, some studies have found that traditional Chinese medicine compounds can exert central neuroprotection by alleviating peripheral inflammation [45]. Therefore, whether YHD can regulate the interaction between peripheral and brain immune systems in AD disease will be one of our future research. In addition, we need to further study the effective components of YHD in reducing inflammation by using serum or cerebrospinal fluid. In addition, the targeted brain tissue drug delivery system has become a feasible therapeutic strategy for AD [46], and with the application of this system, the efficacy of YHD could be further improved.

5. Conclusion

From the perspective of inflamma-aging, by in vitro and in vivo experiments, we found that YHD could regulate the TREM2/NF-κB

signaling pathway through TREM2, thereby regulating MG polarization and reduce neuroinflammation, and finally delaying learning and memory decline of AD at the early stage of aging (Fig. 8).

Ethics statement

The animal experiment was approved by the local ethical committee in the Tianjin University of Traditional Chinese Medicine (TCM-LAEC2020105).

CRediT authorship contribution statement

Kai Wang: Writing – review & editing. **Shujie Zan:** Writing – original draft, Formal analysis, Data curation. **Jiachun Xu:** Writing – original draft. **Weiming Sun:** Writing – original draft, Conceptualization. **Caixia Li:** Writing – review & editing. **Wei Zhang:** Writing – original draft, Data curation. **Daoyan Ni:** Writing – original draft, Data curation. **Ruzhen Cheng:** Software, Methodology. **Lin Li:** Software, Methodology. **Zhen Yu:** Software, Data curation. **Linlin Zhang:** Methodology. **Shuang Liu:** Data curation. **Yuanwu Cui:** Writing – review & editing, Project administration. **Yulian Zhang:** Writing – review & editing, Writing – original draft, Project administration, Methodology.

Declaration of competing interest

The authors declare that they have no known competing financial interests or personal relationships that could have appeared to influence the work reported in this paper.

Acknowledgments

This work is supported by the National Natural Science Foundation of China (Grant Numbers: 81973797, 82104801), and Natural Science Foundation of Tianjin, Tianjin, China. (Grant Number: 19JCQNJC10700).

Appendix A. Supplementary data

Supplementary data to this article can be found online at https://doi.org/10.1016/j.heliyon.2024.e35800.

References

[1] F.T. Hane, B.Y. Lee, Z. Leonenko, Recent progress in Alzheimer's disease research, Part 1: pathology, J Alzheimers Dis 57 (1) (2017) 1–28.
[2] R. Corpas, A.M. Hernandez-Pinto, D. Porquet, C. Hernandez-Sanchez, F. Bosch, A. Ortega-Aznar, et al., Proinsulin protects against age-related cognitive loss through anti-inflammatory convergent pathways, Neuropharmacology 123 (2017) 221–232.
[3] V. Calsolaro, P. Edison, Neuroinflammation in Alzheimer's disease: current evidence and future directions, Alzheimers Dement 12 (6) (2016) 719–732.
[4] S. Bradburn, C. Murgatroyd, N. Ray, Neuroinflammation in mild cognitive impairment and Alzheimer's disease: a meta-analysis, Ageing Res. Rev. 50 (2019) 1–8.
[5] M.T. Heneka, M.J. Carson, K.J. El, G.E. Landreth, F. Brosseron, D.L. Feinstein, et al., Neuroinflammation in Alzheimer's disease, Lancet Neurol. 14 (4) (2015) 388–405.
[6] C. Ising, C. Venegas, S. Zhang, H. Scheiblich, S.V. Schmidt, A. Vieira-Saecker, et al., NLRP3 inflammasome activation drives tau pathology, Nature 575 (7784) (2019) 669–673.
[7] T.A. Pascoal, A.L. Benedet, N.J. Ashton, M.S. Kang, J. Therriault, M. Chamoun, et al., Microglial activation and tau propagate jointly across Braak stages, Nat Med 27 (9) (2021) 1592–1599.
[8] F. Cornejo, R. von Bernhardi, Age-dependent changes in the activation and regulation of microglia, Adv. Exp. Med. Biol. 949 (2016) 205–226.
[9] R. Businaro, M. Corsi, R. Asprino, C. Di Lorenzo, D. Laskin, R.M. Corbo, et al., Modulation of inflammation as a way of delaying Alzheimer's disease progression: the diet's role, Curr. Alzheimer Res. 15 (4) (2018) 363–380.
[10] W. Peng, Y. Xie, C. Liao, Y. Bai, H. Wang, C. Li, Spatiotemporal patterns of gliosis and neuroinflammation in presenilin 1/2 conditional double knockout mice, Front. Aging Neurosci. 14 (2022) 966153.
[11] R. Guerreiro, A. Wojtas, J. Bras, M. Carrasquillo, E. Rogaeva, E. Majounie, et al., TREM2 variants in Alzheimer's disease, N. Engl. J. Med. 368 (2) (2013) 117–127.
[12] T. Jonsson, H. Stefansson, S. Steinberg, I. Jonsdottir, P.V. Jonsson, J. Snaedal, et al., Variant of TREM2 associated with the risk of Alzheimer's disease, N. Engl. J. Med. 368 (2) (2013) 107–116.
[13] Y. Wang, Y. Lin, L. Wang, H. Zhan, X. Luo, Y. Zeng, et al., TREM2 ameliorates neuroinflammatory response and cognitive impairment via PI3K/AKT/FoxO3a signaling pathway in Alzheimer's disease mice, Aging (Albany NY) 12 (20) (2020) 20862–20879.
[14] T.T. Rohn, The triggering receptor expressed on myeloid cells 2: "TREM-ming" the inflammatory component associated with Alzheimer's disease, Oxid. Med. Cell. Longev. 2013 (2013) 860959.
[15] W. Sun, Y. Cui, K. Wang, W. Guo, R. Cheng, Y. Zhang, Effects of yishen Huazhuo decoction on learning and memory ability, hippocampal neurons and expressions of inflammatory factors in senescence accelerated mouse prone 8, Chinese Journal of Information on TCM 26 (7) (2019) 60–65.
[16] K. Wang, W. Sun, J. Xu, Q. Qin, Z. Yu, R. Cheng, et al., Yishen Huazhuo decoction induces autophagy to promote the clearance of abeta$_{1\text{-}42}$ in SAMP8 mice: mechanism research of a traditional Chinese formula against Alzheimer's disease, CNS Neurol. Disord.: Drug Targets 19 (4) (2020) 276–289.
[17] M. Shi, Y. Gong, M. Wu, H. Gu, J. Yu, F. Gao, et al., Downregulation of TREM2/NF-small ka, CyrillicB signaling may damage the blood-brain barrier and aggravate neuronal apoptosis in experimental rats with surgically injured brain, Brain Res. Bull. 183 (2022) 116–126.
[18] T. Fulop, A. Larbi, G. Dupuis, A. Le Page, E.H. Frost, A.A. Cohen, et al., Immunosenescence and inflamm-aging as two sides of the same coin: friends or foes? Front. Immunol. 8 (2017) 1960.

[19] J.R. Conde, W.J. Streit, Microglia in the aging brain, J. Neuropathol. Exp. Neurol. 65 (3) (2006) 199–203.
[20] M.L. Block, Neuroinflammation: modulating mighty microglia, Nat. Chem. Biol. 10 (12) (2014) 988–989.
[21] D.J. DiSabato, N. Quan, J.P. Godbout, Neuroinflammation: the devil is in the details, J. Neurochem. 139 (Suppl 2) (2016) 136–153. Suppl 2.
[22] J.E. Morley, S.A. Farr, V.B. Kumar, H.J. Armbrecht, The SAMP8 mouse: a model to develop therapeutic interventions for Alzheimer's disease, Curr. Pharmaceut. Des. 18 (8) (2012) 1123–1130.
[23] I. Akiguchi, M. Pallas, H. Budka, H. Akiyama, M. Ueno, J. Han, et al., SAMP8 mice as a neuropathological model of accelerated brain aging and dementia: toshio Takeda's legacy and future directions, Neuropathology 37 (4) (2017) 293–305.
[24] A. Fernandez, E. Quintana, P. Velasco, B. Moreno-Jimenez, B. de Andres, M.L. Gaspar, et al., Senescent accelerated prone 8 (SAMP8) mice as a model of age dependent neuroinflammation, J. Neuroinflammation 18 (1) (2021) 75.
[25] Y. Yang, S. Li, H. Huang, J. Lv, S. Chen, D.A.C. Pires, et al., Comparison of the protective effects of ginsenosides Rb1 and Rg1 on improving cognitive deficits in SAMP8 mice based on anti-neuroinflammation mechanism, Front. Pharmacol. 11 (2020) 834.
[26] B. Liu, J. Liu, J.S. Shi, SAMP8 mice as a model of age-related cognition decline with underlying mechanisms in Alzheimer's disease, J Alzheimers Dis 75 (2) (2020) 385–395.
[27] A.W. Corona, A.M. Fenn, J.P. Godbout, Cognitive and behavioral consequences of impaired immunoregulation in aging, J. Neuroimmune Pharmacol. 7 (1) (2012) 7–23.
[28] H.Z. Long, Z.W. Zhou, Y. Cheng, H.Y. Luo, F.J. Li, S.G. Xu, et al., The role of microglia in Alzheimer's disease from the perspective of immune inflammation and iron metabolism, Front. Aging Neurosci. 14 (2022) 888989.
[29] Y.W. Cheng, C.C. Chang, T.S. Chang, H.H. Li, H.C. Hung, G.Y. Liu, et al., Abeta stimulates microglial activation through antizyme-dependent downregulation of ornithine decarboxylase, J. Cell. Physiol. 234 (6) (2019) 9733–9745.
[30] J. Zhang, Y. Zheng, Y. Luo, Y. Du, X. Zhang, J. Fu, Curcumin inhibits LPS-induced neuroinflammation by promoting microglial M2 polarization via TREM2/TLR4/NF-kappaB pathways in BV2 cells, Mol. Immunol. 116 (2019) 29–37.
[31] L. Hamelin, J. Lagarde, G. Dorothee, C. Leroy, M. Labit, R.A. Comley, et al., Early and protective microglial activation in Alzheimer's disease: a prospective study using 18F-DPA-714 PET imaging, Brain 139 (Pt 4) (2016) 1252–1264.
[32] A. Okello, P. Edison, H.A. Archer, F.E. Turkheimer, J. Kennedy, R. Bullock, et al., Microglial activation and amyloid deposition in mild cognitive impairment: a PET study, Neurology 72 (1) (2009) 56–62.
[33] D.M. Norden, J.P. Godbout, Review: microglia of the aged brain: primed to be activated and resistant to regulation, Neuropathol. Appl. Neurobiol. 39 (1) (2013) 19–34.
[34] A. Niraula, J.F. Sheridan, J.P. Godbout, Microglia priming with aging and stress, Neuropsychopharmacology 42 (1) (2017) 318–333.
[35] T. Wyss-Coray, L. Mucke, Ibuprofen, inflammation and Alzheimer disease, Nat Med 6 (9) (2000) 973–974.
[36] G.P. Lim, F. Yang, T. Chu, P. Chen, W. Beech, B. Teter, et al., Ibuprofen suppresses plaque pathology and inflammation in a mouse model for Alzheimer's disease, J. Neurosci. 20 (15) (2000) 5709–5714.
[37] L.K. Huang, Y.C. Kuan, H.W. Lin, C.J. Hu, Clinical trials of new drugs for Alzheimer disease: a 2020-2023 update, J. Biomed. Sci. 30 (1) (2023) 83.
[38] Y.S. Batarseh, Q.V. Duong, Y.M. Mousa, S.B. Al Rihani, K. Elfakhri, A. Kaddoumi, Amyloid-beta and astrocytes interplay in amyloid-beta related disorders, Int. J. Mol. Sci. 17 (3) (2016) 338.
[39] Y. Gao, S. Li, Y. Zhang, J. Zhang, Y. Zhao, C. Chang, et al., Cattle encephalon glycoside and ignotin attenuates abeta1-42-mediated neurotoxicity by preventing NLRP3 inflammasome activation and modulating microglial polarization via TLR4/NF-kappaB signaling pathway, Neurotox. Res. 40 (6) (2022) 1802–1811.
[40] H. Long, G. Zhong, C. Wang, J. Zhang, Y. Zhang, J. Luo, et al., TREM2 attenuates abeta1-42-mediated neuroinflammation in BV-2 cells by downregulating TLR signaling, Neurochem. Res. 44 (8) (2019) 1830–1839.
[41] F. Filipello, R. Morini, I. Corradini, V. Zerbi, A. Canzi, B. Michalski, et al., The microglial innate immune receptor TREM2 is required for synapse elimination and normal brain connectivity, Immunity 48 (5) (2018), 979-91.e8.
[42] Y. Zhang, S. Feng, K. Nie, Y. Li, Y. Gao, R. Gan, et al., TREM2 modulates microglia phenotypes in the neuroinflammation of Parkinson's disease, Biochem. Biophys. Res. Commun. 499 (4) (2018) 797–802.
[43] I.M. Rea, D.S. Gibson, V. McGilligan, S.E. McNerlan, H.D. Alexander, O.A. Ross, Age and age-related diseases: role of inflammation triggers and cytokines, Front. Immunol. 9 (2018) 586.
[44] C. Li, B. Zhao, C. Lin, Z. Gong, X. An, TREM2 inhibits inflammatory responses in mouse microglia by suppressing the PI3K/NF-kappaB signaling, Cell Biol. Int. 43 (4) (2019) 360–372.
[45] Y. Wu, H. Liu, Y. Wang, H. Sheng, Z. Chen, D. Xun, et al., DiHuangYin decoction protects dopaminergic neurons in a Parkinson's disease model by alleviating peripheral inflammation, Phytomedicine 105 (2022) 154357.
[46] Z. Zhu, L. Liao, H. Qiao, Extracellular vesicle–based drug delivery system boosts phytochemicals' therapeutic effect for neurodegenerative diseases 2 (4) (2022) 229–239.